Heterogeneous photocatalysis of butanol and methyl ethyl ketone-characterization of catalyst and dynamic study

Pierre Monneyron, Marie-Hélène Manero, Jean-Noël Foussard, Florence Benoît-marquié, Marie-Thérèse Maurette

Heterogeneous photocatalysis of butanol and methyl ethyl ketone—characterization of catalyst and dynamic study

P. Monneyron[b], M.-H. Manero[b], J.-N. Foussard[b], F. Benoit-Marquié[a], M.-T. Maurette[a,*]

[a] *Université Paul Sabatier, Laboratoire des Interactions Moléculaires et Réactivité Chimique et Photochimique, 118, route de Narbonne, 31062 Toulouse, France*

[b] *Institut National des Sciences Appliquées, Laboratoire d'Ingénierie des Procédés de l'Environnement, 135, avenue de Rangueil, 31077 Toulouse, France*

Abstract

New titanium dioxide (TiO_2) based catalysts were prepared by impregnating commercial zeolites in pellets form using a sol–gel technique. Characterization was done with chemical analysis, X-Ray diffraction, scanning electron microscopy, and BET measurements, together with volatile organic compounds (VOC) adsorption equilibrium experiments. TiO_2 happened to fix on the inert binder leading to a close intimacy of mixing with the zeolites crystallites, without significant modification of support properties. A diffusion cell was used to produce dilute polluted air streams for dynamic experiments, in which adsorption and photodegradation phases were alternatively carried out. Regeneration of adsorbent was evaluated regarding experimental conditions. Through a comparison with the results obtained on impregnated mesoporous borosilicate beads, it was clarified that zeolite supports had no effect on 1-butanol (BuOH) photooxidation mechanisms. Yet, evidence for mass transfer limitation was found, and attributed to intracrystalline diffusion in zeolites.

Keywords: Adsorption; Photochemistry; VOC; High silica zeolites; TiO_2; Diffusion

1. Introduction

Volatile organic compounds (VOC) are major air pollutants coming largely from industrial processes. Thus, purification of effluents is of great interest for chemical engineering, and one of the main techniques available towards dilute polluted airstreams is adsorption onto a porous material. This process is usually conducted in two steps, since the saturated material requires regeneration (Le Cloirec, 1998; Salden & Eigenberger, 2001). Alternatively, photooxidation of air pollutants has been largely developed using the classical UV-sensible catalyst, titanium dioxide (TiO_2) (Ollis, 1993; Legrini, Oliveros, & Braun, 1993). Most of the current wide interest in using TiO_2 in catalytic studies stems from the highly reactive radicals ($OH^{\bullet}$ and $O_2^{\bullet -}$) formed when irradiated together with handling facilities (Al-Ekabi, Serpone, Pelizetti, & Minero, 1989). Nevertheless, since TiO_2 is mainly produced in powder form, which is technologically impracticable in continuous engineering processes, many attempts have been made to prepare supported catalysts, using glass beads (Xu & Chen, 1990), fiber glass (Robert, Piscoro, Heintz, & Weber, 1999; Mattews, 1987), silica (Sato, 1988), stainless steel (Zhu, Zhang, Wang, Fu, & Cao, 2001), fiber textile (Ku, Ma, & Shen, 2001), quartz beads (Benoit-Marquié, 1997), honeycomb (Fernandez, et al., 1995), activated carbon (Nozawa, Tanigawa, Hosomi, Chikusa, & Kawada, 2001; Takeda, Iwata, Torimoto, & Yoneyama, 1998), and zeolites (Green & Rudham, 1993). Besides a large adsorption capacity, high silica zeolites (HSZ) exhibit notably a very low dependence on effluent humidity, contrary to activated carbon (Brosillon, Manero, & Foussard, 2001a, b), and on compound's polarity, which may be of particular interest since non-polar molecules hardly adsorb on pure TiO_2. In order to develop enhanced photoactivity of titanium dioxide, investigators elaborated very different methods to support active titanium on zeolites, from simple amalgam of powders through mechanical mixing (Hashimoto et al., 2001) or with papermaking techniques (Ichiura, Kitaoka, & Tanaka, 2000) to chemical vapor deposition (Ding, Hu, Yue, Lu, & Greenfield, 2001), cation exchange (Kim & Yoon, 2001) or direct synthesis (Kang, Park, & Kim, 2002) which tend to create

* Corresponding author. Tel.: +33-5-61-55-69-68; fax: +33-5-61-55-81-55.

E-mail address: maurette@chimie.ups-tlse.fr (M.-T. Maurette).

doi:10.1016/S0009-2509(02)00637-1

Ti–O–Si bonds. In this study, a sol–gel method was used to impregnate zeolites in pellets form, of two well-known structures, faujasite Y and ZSM-5, to be used in the degradation of VOC from industrial waste gas streams. Most of impregnation methods are based on acid-catalyzed sol–gel formation (Anderson, Gieselman, & Xu, 1988) which may alter framework structure of zeolites (Takeda, Torimoto, Sampath, Kuwabata, & Yoneyama,1995), and studies are to define to what extend the support undergo physical or chemical modifications. Here, characterization of new TiO_2-zeolite catalysts was carried out using global elemental analysis, X-ray diffraction, scanning electron microscopy (SEM) with microprobe elemental analysis and BET measurements. Specific adsorption capacity of the different zeolites-based catalysts was appraised toward daily used industrial solvents (1-butanol and 2-butanone). Aiming to close in on industrial effluents conditions, dilute VOC containing gases were generated in a diffusion cell, and then oxidized through dynamic photodegradation experiments. This particular process was also directed towards assessing the efficiency of photocatalysis in terms of adsorbent regeneration.

2. Experimental section

2.1. Chemicals and zeolites supports

Titanium (IV) butoxide (99%), 2,4-pentanedione (99%), 1-butanol (99.5%), and 2-butanone (99.5%) were all purchased from Aldrich, and used without further purification. Absolute ethanol came from ACS for Analysis, RPE, Carlo Erba. The commercial zeolites used in this study were cylindrical pellets (diameter 2 mm, length 5 mm) supplied by Degussa. The granular solids were made of microcrystals of zeolites arranged together with a clay binder (20% weight). Table 1 summarizes the main physical properties of the HSZ used in this study.

2.2. Preparation of supported titanium dioxide catalysts (Bailleux & Benoit-Marquié, 2001)

The catalysts were prepared by impregnation of supports with a TiO_2 sol–gel. The synthesis method is summarized here. 0.1 mole of titanium (IV) butoxide was dissolved in 1 mol of absolute ethanol in an argon atmosphere and refluxed for 12 h. 0.05 mol of 2,4-pentanedione and 0.01 mol of double distilled water were added dropwise under vigorous stirring. After refluxing for several hours, the clear solution was concentrated by solvent distillation. An amorphous and translucid gel was obtained. It contains enough alcohol to avoid aging and could therefore be stored unchanged for several weeks. The TiO_2 coating was made by completely immersing the different supports in the gel. The wet materials could then undergo a two-step hot air treatment. In the first stage the catalyst system was dried at 100°C, whereas in the second part the desired crystalline anatase phase was obtained at 450°C. From now on, the DAY (resp. DAZ) based catalysts are referred as DAY* (resp. DAZ*).

2.3. Physical and chemical characterization of catalysts

Elemental analysis was performed by the analysis central center of the Centre National de la Recherche Scientifique (CNRS) using flame emission spectrometry. The titanium crystallized phase obtained after the thermal treatment was identified by X-ray diffraction, with an automatic diffractometer (Seifert XRD3003TT). Diffraction of the Kα radiations emitted by Copper ($\lambda_1 = 1.5406$ Å and $\lambda_2 = 1.5444$ Å) was analyzed for 2θ varying between 20° and 50° with a scan time of 4 s/0.02°. The specific surface area and porous distribution of adsorbents were determined using argon adsorption-desorption experiments at 77 K, using a conventional BET adsorption apparatus (ASAP 2010, Micrometrics). Degassing of samples was performed at 120°C overnight. This equipment allowed the description of both microporosity (pore size smaller than 2 nm) and mesoporosity (between 2 and 50 nm). A scanning electron microscopy (JSM-840 A, JEOL) was operated at 20 keV, providing information on local properties together with chemical composition of material activated by electronic bombardment (EDS facility). Prior to analysis, the granulates were coated with gold to ensure conductivity. Both external and cross-section surfaces of samples were analyzed. In order to characterize the influence of impregnation on adsorption capacities of zeolites, batch adsorption isotherms were performed using a volumetric method (Brosillon, Manero, & Foussard, 2001a, b). The adsorbent was introduced into an atmosphere polluted by liquid VOC injection, followed by evaporation; adsorption occurred at a fixed temperature (20°C). Once equilibrium time was reached (2 h), analysis of the gas phase was carried out with a Hewlett-Packard gas chromatograph (HP 5890 II).

Table 1
Main properties of adsorbents

Symbol	Crystalline type (pore structure)	Si/Al ratio	Available porous volume ($cm^3\ g^{-1}$)
DAY	Faujasite Y (α-cage)	> 100	0.30
DAZ	ZSM-5 (interconnected channels)	> 500	0.19

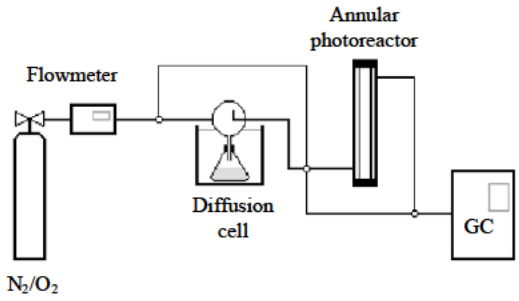

Fig. 1. Experimental setup of dynamic adsorption/photooxidation cycles.

2.4. Gas phase adsorption/photocatalysis experiments

Fig. 1 presents the setup used for dynamic photocatalysis experiments. The polluted air stream was generated with a diffusion cell (McKelvey & Hoelscher, 1957), which can produce dilute gas mixtures accurately for very long period of time. The diffusion rate initially expressed by the Altshuller and Cohen equation was used in a previous study (Benoit-Marquié, et al., 2000b) for the prediction of the experimental temperature-dependent relation, using Antoine equation to estimate the vapor pressure of liquid, and Fuller relation for diffusion coefficient calculation. Here, a 80:20 N_2/O_2 mixture, supplied by Air Liquide, continuously flushed the mixing reservoir, regulated by a mass flowmeter (Brooks 58505, 10–50 ml min^{-1}), leading to a VOC concentration ranging between 300 and 5000 mg m^{-3}, thermally controlled. Both adsorption and irradiation cycles were carried out in a continuous flow annular reactor (length: 15 cm, optical path length: 3 mm, total volume: 60 cm^3). A medium pressure mercury arc (Phillips HPK 125 W, photonic rate: 1.62×10^{29} photon s^{-1}) was positioned in the internal cylinder, entirely made of Pyrex to avoid photolysis of compounds, and cooled with an air stream. The fixed bed of catalysts was supported by means of a non-porous quartz cloth inserted in the annular space and, with a typical mass of 2 g, a homogeneous bed height of about 1 cm was obtained. The on-line reactor outlet analysis was performed using a Chrompack CP900 gas chromatograph.

3. Results and discussion

3.1. Physical and chemical characterization of TiO_2-zeolites catalysts

3.1.1. Chemical analysis

The reproducibility of impregnation was checked by evaluating the gain of mass from TiO_2 coating through a simple and rapid weighting method. The TiO_2 mass content of DAY* and DAZ* was, respectively, 16$ and 15%. Elemental quantification confirmed the accuracy of these findings, with a titanium content of 9% for DAY* and 10% for DAZ*.

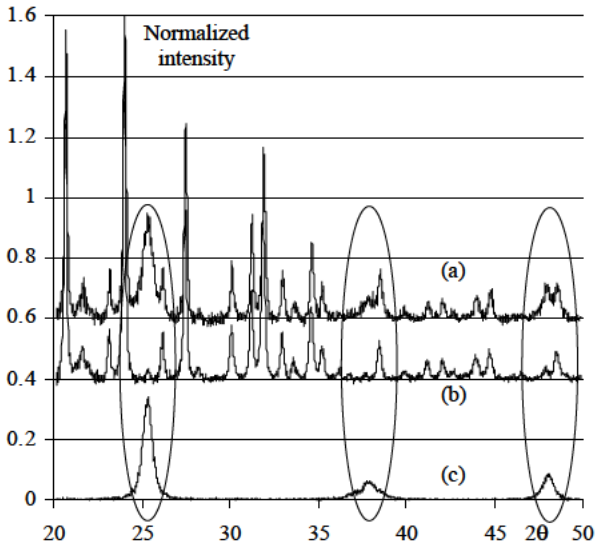

Fig. 2. XRD spectrum of DAY* catalyst. (a) Coated DAY*, (b) Uncoated DAY, and (c) SGP.

3.1.2. X-Ray diffraction analysis (XRD)

The efficiency of photooxidation depends greatly on titanium dioxide crystalline form, anatase being much more UV sensible than rutile, and required examinations of the unsupported TiO_2 powder synthesized with the sol–gel technique (called SGP from now on), and also of loaded and unloaded catalysts. Prior to any investigations of TiO_2 crystalline form, the quantitative ratio of anatase and rutile crystalline form of P25 (the well-known TiO_2powder supplied by Degussa) was checked (80:20). The SGP spectrum exhibited only anatase specific peaks, indicating that contrary to other sol–gel methods (Xu & Langford, 1995) no rutile crystals was formed. In this study, only high TiO_2 mass content catalyst were prepared, but it is interesting to note that other researchers demonstrated that at low coverage of zeolite powder (1–5% of TiO_2 in mass), oxides of titanium were amorphous whereas approach anatase crystals at high coverage (Xu & Langford, 1995; Zhu et al., 2000). The results obtained for the two supported catalysts, DAZ* and DAY*, were very similar. Fig. 2 presents an apparently complex spectrum, obtained for DAY*. Nevertheless, this complexity came from the zeolites structure, and a perfect correlation of the loaded catalysts graph (a) was obtained by adding to the uncovered support's spectrum (b) a relative amount of the SGP pattern (c), as highlighted in circled areas.

These results confirm that using a support or not does not influence the TiO_2 crystalline form. XRD analysis indicates that no change in the typical morphology of the support happened during titanium loading, suggesting that TiO_2 linked with the amorphous binder. These findings are significantly different from Takeda work (1995) that noticed a framework alteration when using an acid-catalyzed sol–gel on zeolites A, with a low Si/Al ratio.

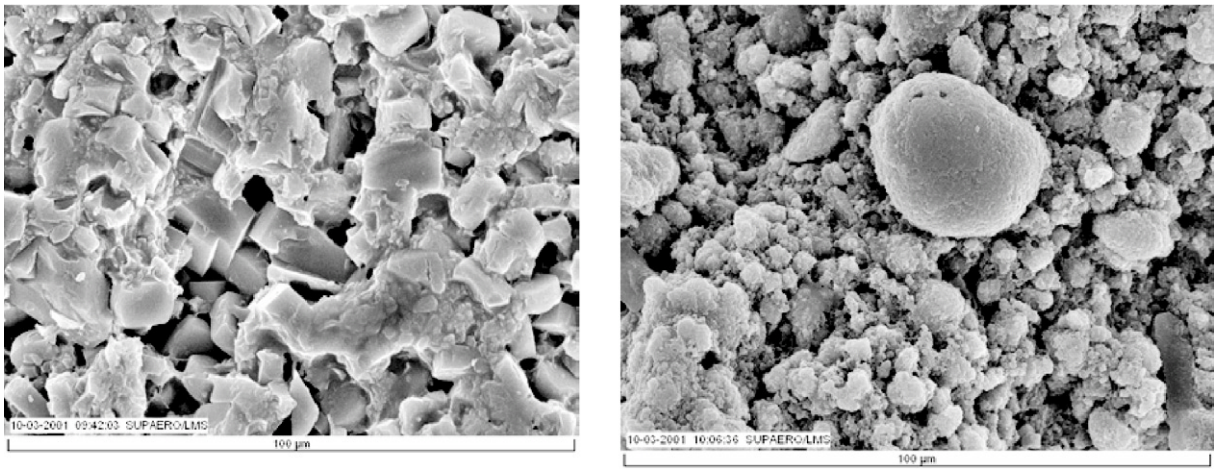

Fig. 3. SEM pictures (G = 1200) of internal surface. DAZ* (left), DAY* (right).

Table 2
Specific surface area of catalysts

Adsorbent	Specific surface area of adsorbent[a] ($m^2\ g^{-1}$)	Specific surface area of TiO_2-loaded adsorbent[b] ($m^2\ g^{-1}$)	Calculated surface area of mixture[c] ($m^2\ g^{-1}$)
SGP	65		
DAY	645	568	566
DAZ	379	337	336

[a]Zeolites adsorbent have a binder mass content of 20%.
[b]The composition of catalysts is zeolite-binder—TiO_2 (69:16:15).
[c]The calculated value of surface area was done considering that the surface area of adsorbent came only from zeolites crystals, and consequently, by normalizing the surface areas with the zeolite mass content. Expression of calculation is then [$S_{Calc} = (S_{Ads}/0.80) \times 0.69 + S_{SGP} \times 0.15$].

3.1.3. SEM-EDS analysis

Characterization of intimacy and homogeneity of TiO_2 loading is of primary importance for further investigations and understanding of catalysts photoactivity. Results of external and cross-section surfaces where very similar in terms of mixing and titanium content, determined through Si/Ti ratio calculations. Fig. 3 shows SEM pictures of cross-section surfaces for the two catalysts.

On the DAZ* sample, the zeolites crystallites can be easily isolated via their rectangular shape. Using the microprobe elemental analysis (EDS), no titanium was detected on the zeolites crystals whereas a high content of titanium was found in the clearer irregular parts, mixing TiO_2 microcrystals and binder, strengthening the XRD analysis conclusions. The DAY* structure is quite different from DAZ*. The zeolites crystals are much smaller and they could not be distinguished from binder or TiO_2, showing a greater intimacy of loading during sol–gel method. Homogeneity of catalysts was found to be fairly satisfactory, and strongly determined by the initial material, and zeolite crystals size.

3.1.4. BET analysis

BET adsorption isotherms on the different samples were all of type Ia of IUPAC classification (IUPAC Physical Chemistry Division, 1985), corresponding to a microporous adsorbent with a small hysteresis coming from multilayer adsorption/desorption in mesopores. Microporous distribution was checked using Horvath–Kawazoe model extended by Saïto and Foley for a cylindrical pore geometry. Structures of zeolites were confirmed, with a monomodal porous distribution for faujasite Y, at 13.8 Å and bimodal for ZSM-5, at 10.0 and 12.6 Å. The modification of support's surface due to TiO_2 loading was investigated by two means. First, the surface area of catalysts where determined with Langmuir approach as shown in Table 2. This model was preferred to BET or Dubinin–Radushkevich equation considering the monomolecular adsorption taking place in microporous adsorbent.

The very good agreement between experimental and calculated surface areas confirms that TiO_2 loading does not change greatly the support physical properties. Aiming to supplement this conclusion, BJH model was used to study adsorption isotherms desorption parts. To understand coating's influence on mesoporous distribution of supports, the differential volumes given in Fig. 4 have been normalized according to zeolite mass content, representative of the unchanged number of pellets.

The global mesoporous volume of DAY is much larger than DAZ one. On both adsorbents, the TiO_2 coating developed a noticeable porous volume. Since the gel

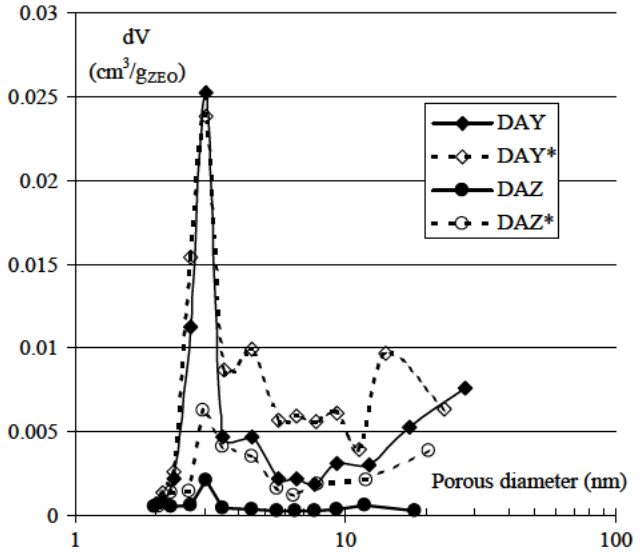

Fig. 4. TiO_2 loading influence on mesoporous volume distribution of catalysts.

actually penetrated the pellets, and was then expected to reduce the porous volume, the previous observation could be ascribed to different factors. It remains unclear whether this mesoporous volume increase came from a modification of the macroporous structure, leading to narrower pores or from a volume development happening on the external surface. Yet, these observations stand promising for photocatalytic experiments, mesopores being predominant sites for photocatalysis.

3.1.5. *VOC adsorption isotherms*

Single component adsorption isotherms of BuOH and MEK were realized on naked and coated adsorbents, and on TiO_2 powder (SGP). Representative results are given in Fig. 5, using semi-logarithmic scale for clearer presentation, p_0 being vapor pressure of VOC.

BuOH and MEK exhibit a significant deviation when adsorbed on SGP at very low pressure, as shown in Fig. 5a. This stronger affinity of TiO_2 for BuOH than for MEK is readily explained by the electrostatic interactions between TiO_2 and BuOH hydroxyl groups. Still, for higher pressure their maximum capacity reached about the same value (0.25 mmol g^{-1}), which is significantly smaller than the pure zeolites maximum adsorption capacities when comparing with the results of Fig. 5b for BuOH. For the two VOC used in this study, no steric effect happened, and the maximum adsorption capacity for the two zeolites was then directly proportional to the available pore volume given in Table 1. The two compounds show very similar adsorption mechanisms on zeolites. As can be seen on Fig. 5b for BuOH, the isotherm shapes were respectively of type I (IUPAC Physical Chemistry Division, 1985) for ZSM-5 and of type V (or 'S'-shape) for faujasite Y representative of a favorable desorption (Rouquerol, Rouquerol, & Sing, 1999), the low pressure part of isotherm being driven by chemisorption on extra-framework strong acid sites (Boréave, Auroux, & Guimon, 1997). For both zeolites, the TiO_2 loading reduces the maximum adsorption capacity proportionally to the TiO_2 mass content: the isotherms obtained on the different DAY-based catalysts, DAY* (16%) and DAY* (27%), are testimonies to this adsorption behavior. Adsorption isotherms determination was instrumental in demonstrating unequivocally that VOC adsorption on synthesized catalysts is almost completely driven by the volume of zeolite micropores, which are totally left unobstructed by TiO_2 loading, contrary to the BET results obtained by Hsien, Chang, Chen, and Cheng (2001) when impregnating zeolite powders.

3.2. *Heterogeneous catalysis for waste-air treatment*

3.2.1. *Dilute VOC air stream generation*

The diffusion cell technique naturally requires experimental calibration, and here a comparison with predicted diffusion rate was done. In the Fuller equation, the diffusion coefficient is proportional to (T^m), where m is usually 2, and may be 1.75 (Debbrecht, Daugherty, & Neel, 1979). When fitting experimental data, m was found to be equal to 1.75 for BuOH and 2 for MEK. Results of both prediction and

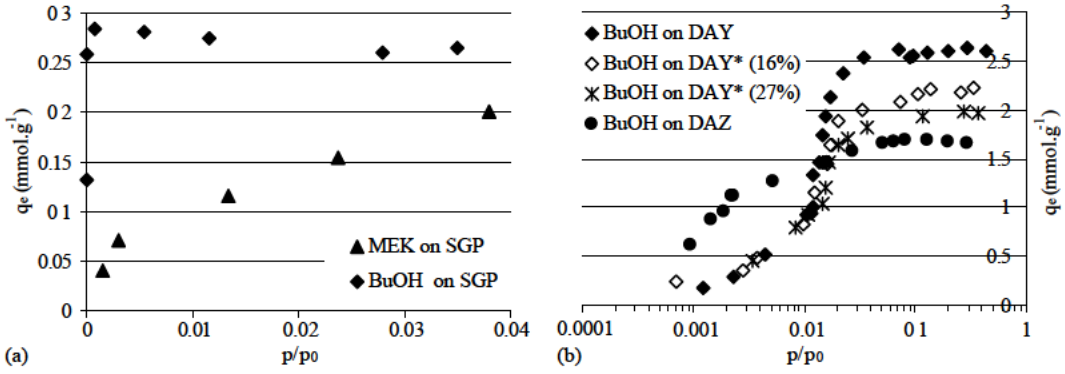

Fig. 5. Single component adsorption isotherms. (a) BuOH and MEK on SGP, and (b) BuOH on different adsorbents.

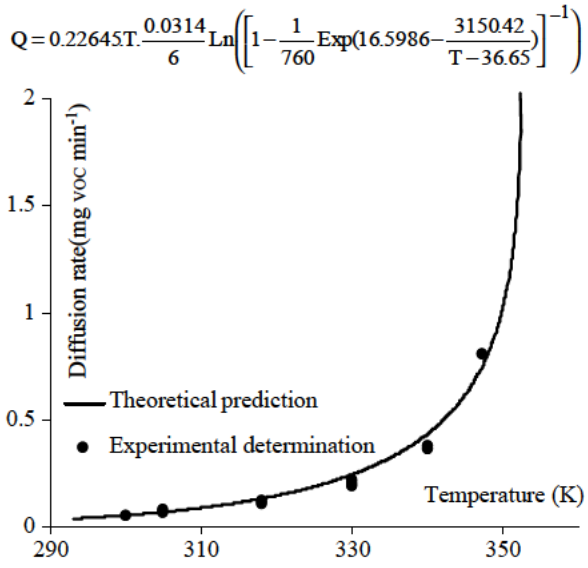

Fig. 6. Diffusion cell experimental calibration for MEK—A comparison with theoretical prediction.

experimental data for MEK are given in Fig. 6, together with the reduced Altshuller equation for a 2.0 mm bore and 6.0 cm in length diffusion tube. Deviation were found to be smaller than 5% in the temperature range studied and therefore theoretical equation was used to set the inlet VOC concentration in dynamic experiments.

3.2.2. Cyclic adsorption/photocatalytic oxidation dynamic experiments

Dynamic gas phase experiments were carried out in a single reactor, shifting from adsorption to oxidation phase just by turning the mercury lamp on once breakthrough curve was totally described and adsorbent saturation completed. The VOC inlet concentration was kept unchanged during irradiation, which was interrupted as soon as the outlet concentration of VOC became still. This choice lead one to analyze final adsorption/photochemical steady state instead of complete regeneration time which may be uneasy to characterize considering the complex mechanisms involved in this process. Efficiency of degradation was then estimated in terms of outlet to inlet concentration ratio. Fig. 7 presents the outlet concentration of the reactor versus time during the cyclic study of adsorption breakthrough curves (A) followed by photocatalytic phase (P) of BuOH on DAY* for an inlet concentration of 550 mg m^{-3}.

Several preliminary remarks are to be made. Due to a great temperature dependence of the adsorption mechanism, fluctuations can be observed in each of the three adsorption periods, coming from laboratory temperature change during night and day, of about ±2°C. In the same way, a thermodesorption was observed when initializing irradiation phase. Photocatalysis lead to significant degradation of BuOH, consecutively 94% and 93%. Regeneration of adsorption

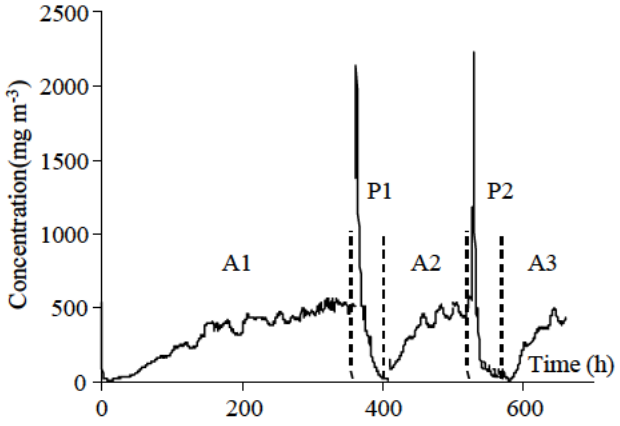

Fig. 7. Cyclic study of adsorption/photodegradation of BuOH on DAY*.

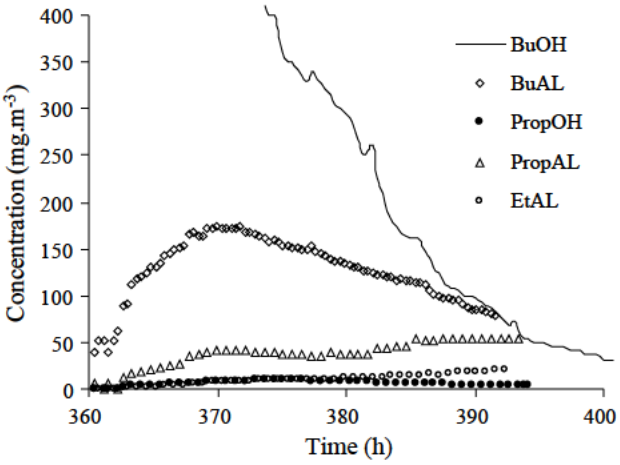

Fig. 8. Outlet content during the irradiation phase of saturated DAY* (C_{inlet} = 550 mg m^{-3}).

capacity was estimated by comparing the saturation time of adsorbent before and after the irradiation. In both cases, a partial regeneration was found of about 30%. This value is totally dependent on the experimental conditions (experimental setup design, irradiation conditions, inlet concentration and flow) and also on the competitive mechanisms of photochemical reactions, adsorption and desorption of VOC. Still, this value remaining constant indicates that no poisoning of catalysts occurred when irradiated. In Fig. 8, the outlet evolution of BuOH oxidation sub-products concentration is presented, focusing on the first photodegradation since identical shapes of curves were obtained during the second phase. Each of them was identified by direct injection of its vapor.

C-4 to C-2 alcohols (noted _OH) and corresponding aldehydes (noted _AL) were detected in the outlet during all the irradiation period. The evolution of their concentration had a very similar tendency to those obtained in a previous study on loaded silica beads in similar conditions by Benoit-Marquié, Boisdon, Braun, Oliveros, and Maurette

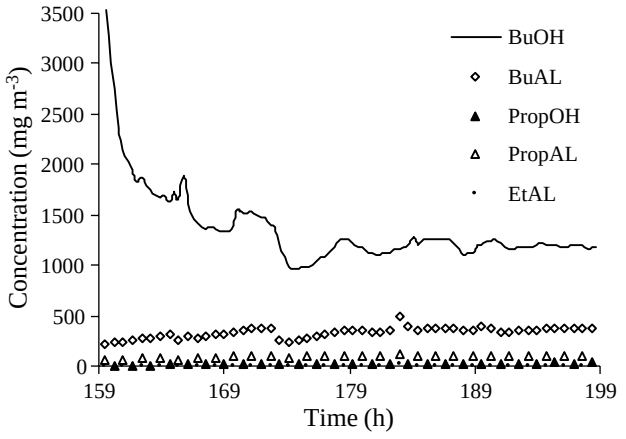

Fig. 9. Outlet content during the irradiation phase of saturated DAZ* ($C_{inlet} = 2000$ mg m^{-3}).

(2000a). The greater affinity of TiO_2 toward alcohols due to their hydroxyl group interactions is to explain why aldehydes outlet concentration was greater than the corresponding alcohol one. The adsorption isotherms on SGP presented in Fig. 5a support this interpretation. These findings tend to indicate that the zeolite used in this study does not interfere with the oxidative mechanisms that occur on the active TiO_2 UV-sensible sites; the unloaded zeolites had no catalytic properties when irradiated in identical conditions. Supporting TiO_2 on zeolites may have two different impacts on photocatalysis reactions: firstly, it is clear that by creating a high concentration of compounds around TiO_2 sites, kinetic rates are to increase significantly. This phenomenon was observed in batch experiments by many researchers (Sampath, Uchida, & Yoneyama, 1994; Chen et al., 1999). Secondly, the zeolites, being acid material, may influence selectivity of reactions through chemisorption on Lewis or Brönsted strong acid sites, induced by aluminum atoms (Brueva, Mishin, & Kapustin, 2001; Beaune et al., 1993). Here, the impact of acidity on oxidation rate remains unclear but may tend to reduce mass transfer between external adsorption sites, and TiO_2 sites. The same study was performed with a BuOH inlet concentration of 2000 mg m^{-3}, leading to similar sub-products curves, but to a different degradation steady state of 75%, which can be easily explained by the competitive adsorption and photodegradation mechanisms. Finally, the DAZ* catalyst was studied with a 2000 mg m^{-3} inlet concentration: irradiation lead very rapidly to a steady state of 40% of degradation, but only a very small adsorbent regeneration was obtained (about 5%). The outlet gas content obtained during the first irradiation phase is presented in Fig. 9.

When beginning the irradiation phase, a smaller thermodesorption was observed compared with the DAY* experiments, confirming that faujasite structure is more favorable to desorption than ZSM-5. Moreover, it should be noticed that the initial slope of BuAL curve is significantly different, the concentration being initially very different from 0. This phenomenon can be explained by the different affinity of zeolites towards alcohol and aldehyde, and may be clarified by further competitive adsorption investigations. These findings clearly illustrate that a mass transfer limitation occurs in zeolite crystals. In this study, two main parameters are distinguishing DAY* and DAZ* catalysts that can explain the differences observed in photocatalysis experiments. Firstly, it is obvious that the zeolite framework structure has a decisive impact, intracrystalline diffusion being faster in faujasite Y than in ZSM-5. Secondly, SEM measurements showed that DAY crystals were smaller than DAZ ones, creating a greater intimacy of mixing and a larger mesoporous volume. Therefore, zeolite crystals size is likely to limit mass transfer in the catalyst. It was not possible to determine here their respective influence, but in both cases, intracrystalline diffusion is the microscopic decisive parameter. By investigating the correlation between adsorption energy and the rate of photodegradation of mixed TiO_2/adsorbent towards propionaldehyde, Yoneyama and Torimoto (2000) also pointed at the major influence of diffusion in adsorbent on heterogeneous photocatalysis efficiency.

4. Conclusions

The zeolites in pellets form used in this study were original supports for a titanium sol–gel impregnation, and physical characterization of materials showed that a great intimacy of mixing was obtained without significant modification of adsorbent. Interestingly, these promising findings unabled us to discuss dynamic experiments, explaining that the zeolites did not interfere with oxidation mechanism of BuOH, and clarifying the decisive role of intracrystalline diffusion in heterogeneous catalysis. These conclusions were essential prior to any investigations on a more light-efficient reactor design adapted to industrial requirements.

Acknowledgements

We would like to thank Degussa for supply of zeolites, Gustave Tayebi for glass work, l'Ecole Nationale Supérieure d'Aeronautique (Toulouse) for SEM experiments, and Midi-Pyrénées Region for financial support.

References

Al-Ekabi, H., Serpone, N., Pelizetti, E., & Minero, C. (1989). *Langmuir*, *5*, 250.

Anderson, M. A., Gieselman, M. J., & Xu, Q. (1988). Titania and aluminia ceramics membranes. *Journal of Membrane Science*, *39*, 243–258.

Bailleux, C., & Benoit-Marquié, F. (2001). Nouveaux réacteurs photocatalytiques à base de dioxyde de titane sur support silice pour le traitement de l'air et de l'eau. French Patent FR 0002923.

Beaune, O., Finiels, A., Geneste, P., Graffin, P., Guida, A., Olivé, J. L., & Saeedan, A. (1993). Selective photocatalytic oxidation of hydrocarbon

compounds over zeolites. In M. Guisnet et al. (Ed.), *Heterogeneous Catalysis and Fine Chemicals III*, 401.

Benoit-Marquié, F. (1997). Ph.D. thesis no 2632, Université Paul Sabatier, Toulouse, France.

Benoit-Marquié, F., Boisdon, M. T., Braun, A. M., Oliveros, E., & Maurette, M.-T. (2000a). Dégradation de composés organiques en phase gazeuse par photocatalyse et par photolyse V-UV. *Entropie*, *228*, 36–43.

Benoit-Marquié, F., Wilkenhöner, U., Simon, V., Braun, A. M., Oliveros, E., & Maurette, M.-T. (2000b). VOC degradation at the gas–solid interface of a TiO_2 photocatalyst. Part I: 1-butanol and 1-butylamine. *Journal of Photochemistry and Photobiology A*, *132*, 225–232.

Boréave, A., Auroux, A., & Guimon (1997). Nature and strength of acid sites in HY zeolites: A multitechnical approach. *Microporous Materials*, *11*, 275–291.

Brosillon, S., Manero, M.-H, & Foussard, J.-N. (2001a). Mass transfer in VOC adsorption on zeolite: Experimental and theoretical breakthrough curves. *Environmental Science and Technology*, *35*, 3571–3575.

Brosillon, S., Manero, M.-H., & Foussard, J.-N. (2001b). *Récents Progrès en Génie des Procédés*, *15*(86), 343.

Brueva, T. R., Mishin, I. V., & Kapustin, G. I. (2001). Distribution of acid-site strengths in hydrogen zeolites and relationship between acidity and catalytic activity. *Thermochimica Acta*, *379*, 15–23.

Chen, H., Matsumoto, A., Nishimiya, N., & Tsutsumi, K. (1999). Preparation and characterization of TiO_2 incorporated Y-zeolite. *Colloids and Surfaces A: Physicochemical and Engineering Aspects, 157*, 295–305.

Debbrecht, F. J., Daugherty D. T., & Neel, E. M. (1979). Diffusion tubes as a primary standard for OSHA-type calibration. *Trace organic analysis: a new frontier in analytical chemistry*: 9*th materials research symposium* (pp. 761–769). Gaithersburg, MD.

Ding, Z., Hu, X., Yue, P. L., Lu, G. Q., & Greenfield, P. F. (2001). Synthesis of anatase TiO_2 supported on porous solids by chemical vapor deposition. *Catalysis Today*, *68*, 173–182.

Fernandez, A., Lassaletta, G., Jimenez, V. M., Justo, A., Gonzalez-Elipe, A. R., Herrmann, J. M., Tahiri, H., & Ait-Ichou, Y. (1995). *Applied Catalysis B*, *7*, 49.

Green, K. J., & Rudham, R. J. (1993). *Chemical Society, Faraday Transactions*, *89*, 1867.

Hashimoto, K., Wasada, K., Osaki, M., Shono, E., Adachi, K., Toukai, N., Kominami, H., & Kera, Y. (2001). Photocatalytic oxidation of nitrogen oxide over titania-zeolite composite catalyst to remove nitrogen oxides in the atmosphere. *Applied Catalysis B*, *30*, 429–436.

Hsien, Y-H., Chang, C-F., Chen, Y-H., & Cheng, S. (2001). Photodegradation of aromatic pollutants in water over TiO_2 supported on molecular sieves. *Applied Catalysis B*, *31*, 241–249.

Ichiura, H., Kitaoka T., & Tanaka, H. (2000). Photocatalytic decomposition of VOC by Zeolite-TiO_2 composite sheet prepared using papermaking technique. *Proceeding on environmentally friendly and emerging technologies for a suitable pulp and paper industry*, Taiwan.

IUPAC Physical Chemistry Division (1985). *Pure and Applied Chemistry 57*(4), 603–619.

Kang, M. G., Park, H. S., & Kim, K.-J. (2002). Effect of improved crystallinity of titanium silicalite-2 on photodecomposition of simple aromatic hydrocarbons. *Journal of Photochemistry and Photobiology A*, to be published.

Kim, Y., & Yoon, M. (2001). TiO_2/Y-Zeolite encapsulating intramolecular charge transfer molecules: A new photocatalyst for photoreduction of methyl orange in aqueous medium. *Journal of Molecular Catalysis A*, *168*, 257–263.

Ku, Y., Ma, C. M., & Shen, Y. S. (2001). *Applied Catalysis B*, *34*, 181–190.

Le Cloirec, P. (1998). *Les composés organiques volatils dans l'environnement*. Paris: Lavoisier Tec. & Doc.

Legrini, O., Oliveros, E., & Braun, A. M. (1993). *Chemical Review*, *93*, 671–698.

Mattews, R. W. (1987). *Solar Energy*, *38*, 405.

McKelvey, J. M., & Hoelscher, H. E. (1957). Apparatus for preparation of very dilute gas mixtures. *Analytic Chemistry*, *29*(1), 123.

Nozawa, M., Tanigawa, K., Hosomi, M., Chikusa, T., & Kawada, E. (2001). *Water Science and Technology*, *44*(9), 127–133.

Ollis, D. F. (1993). *Photocatalytic purification and treatment of water and air*. Lausanne: Elsevier.

Robert, D., Piscoro, A., Heintz, O., & Weber, J. V. (1999). *Catalysis Today*, *54*, 291–296.

Rouquerol, F., Rouquerol, J., & Sing, K. (1999). *Adsorption by powders & porous solids, principles, methodology and applications*. New York: Academic Press.

Salden, A., & Eigenberger, G. (2001). Multifunctional adsorber/reactor concept for waste-air purification. *Chemical Engineering Science*, *56*, 1605–1611.

Sampath, S., Uchida, H., & Yoneyama, H. (1994). Photocatalytic degradation of gaseous pyridine over zeolite-supported titanium dioxide. *Journal of Catalysis*, *149*, 189–194.

Sato, S. (1988). *Langmuir*, *4*, 1156.

Takeda, N., Iwata, N., Torimoto, T., & Yoneyama, H. (1998). Influence of carbon black as an adsorbent used in photocatalyst films on photodegradation behaviors of propyzamide. *Journal of Catalysis*, *177*, 240–246.

Takeda, N., Torimoto, T., Sampath, S., Kuwabata, S., & Yoneyama, H. (1995). Effect of inert supports for titanium dioxide loading on enhancement of photodecomposition rate of gaseous propionaldehyde. *Journal of Physical Chemistry*, *99*, 9986–9991.

Xu, Y., & Chen, X. (1990). *Chemical Industry (London)*, *6*, 497.

Xu, Y., & Langford, C. H. (1995). Enhanced photoactivity of a titanium(IV) oxide supported on ZSM5 and zeolite A at low coverage. *Journal of Physical Chemistry*, *99*, 11501–11507.

Yoneyama, H., & Torimoto, T. (2000). Titanium dioxide/adsorbent hybrid photocatalysts for photodestruction of organic substances of dilute concentrations. *Catalysis Today*, *58*, 133–140.

Zhu, C., Wang, L., Kong, L., Yang, X., Wang, L., Zheng, S., Chen, F., MaiZhi, F., & Zong, H. (2000). Photocatalytic degradation of AZO dyes by supported $TiO_2 + UV$ in aqueous solution. *Chemosphere*, *41*, 303–309.

Zhu, Y., Zhang, L., Wang, L., Fu, Y., & Cao, L. (2001). *Journal of Material Chemistry*, *11*(7), 1864–1868.